Effects of Billet Preheating Temperature on the Microstructure and Operational Reliability of Hot-Forged C45 Steel Horns

Ngoc-Nam Tran
Faculty of Mechanical Engineering, Ho Chi Minh City University of Technology (HCMUT), Ho Chi Minh City, Vietnam | Vietnam National University Ho Chi Minh City, Ho Chi Minh City, Vietnam | Mechanical Workshop, X52 Naval Dockyard, Cam Ranh City, Vietnam
tnnam.sdh231@hcmut.edu.vn

Trung-Kien Le
School of Mechanical Engineering, Hanoi University of Science and Technology, Hanoi, Vietnam
kien.letrung@hust.edu.vn

Thanh-Hai Nguyen
Faculty of Mechanical Engineering, Ho Chi Minh City University of Technology (HCMUT), Ho Chi Minh City, Vietnam | Vietnam National University Ho Chi Minh City, Ho Chi Minh City, Vietnam
haint@hcmut.edu.vn (corresponding author)

Received: 3 September 2025 | Revised: 22 September 2025 and 13 October 2025 | Accepted: 18 October 2025

 DOI: https://doi.org/10.48084/etasr.14510

ABSTRACT

This study examined the effect of billet preheating temperature ranging from 1220 to 1275 ºC on the microstructure and performance of C45 steel ultrasonic horns. Six samples were fabricated and evaluated for microstructure and ultrasonic performance at 28 kHz through DEFORM-3D simulations and experimental forging trials. The unforged sample (Horn 1) exhibited the highest Q_m (3,434), reflecting minimal energy loss under free resonance conditions. However, it failed during ultrasonic operation due to severe local heating and burning at the horn belly, indicating poor thermal reliability. The sample forged at 1,266 ºC (Horn 5) showed refined, Dynamically Recrystallized (DRX) microstructures with reduced anisotropy and stable resonance frequencies close to 28 kHz. These results confirm that billet heating temperature strongly governs both microstructural evolution and acoustic behavior. The optimal preheating temperature of 1266 °C ensures a refined, homogeneous microstructure that provides the necessary mechanical integrity and thermal stability for reliable ultrasonic horn operation.

Keywords-C45 steel; hot forging; billet preheating temperature; ultrasonic welding horn; microstructure evolution; ultrasonic transmission efficiency

I. INTRODUCTION

Ultrasonic technology is widely applied in manufacturing due to the enhanced joining, machining, and forming processes through efficient energy transfer [1]. In ultrasonic welding of dissimilar materials, such as aluminum and copper, the horn plays a decisive role in the weld quality and final microstructure [2]. For Al/CFRTP welding, the bonding strength can be improved through surface modification at the horn-workpiece interface, while the resonance stability and durability of steel horns can be improved through appropriate heat treatments [3, 4]. Research on die steels has introduced alloy optimization and strengthening strategies to meet industrial demands [5]. The hardness of hot forging dies has been correlated with service life [6], whereas thermal fatigue and wear remain major factors limiting tool performance [7]. Die geometry also influences wear resistance and operational stability [8]. Evidence from industrial case studies confirms that die wear is a repeated challenge in forging production [9]. Research has further demonstrated that heat treatment alters the microstructure and mechanical properties of steels [10]. In [11], the thermal analysis conducted showed that the temperature history of tool steels affects their mechanical behavior. Advances in alloy design and modeling approaches (e.g., multilayer steels, neural network predictions) have provided general insights into microstructure optimization [12, 13].

Since the acoustic properties of steels are highly sensitive to temperature [14], the connection between thermal history, microstructural evolution, and acoustic response has been

examined. Investigations on other alloy systems, including high-entropy and AlCo alloys, have also emphasized the role of Dynamic Recrystallization (DRX) for grain refinement during hot working [15-19]. DRX during hot working is essential for grain refinement and strength enhancement [20]. Furthermore, nonlinear ultrasonic testing has been applied to evaluate heterogeneity in forged products [21].

Despite extensive studies on steel forging and ultrasonic horn performance, the examination of billet preheating temperature specifically for C45 ultrasonic horns is still lacking. C45 steel is a widely used material in ultrasonic applications due to its toughness and strength balance. However, improper preheating may cause incomplete recrystallization or coarse grains, which reduce acoustic stability. To address this gap, the present study combines DEFORM-3D simulations with controlled forging experiments to clarify how billet preheating temperature affects both microstructural evolution and ultrasonic performance.

II. EXPERIMENTAL PROCEDURES

A. Materials

This study utilized cylindrical billets of medium carbon steel (C45) due to their favorable combination of strength, hardness, and ultrasonic transmission characteristics after thermal processing (Figure 1). The chemical composition (in wt.%) was approximately 0.45% C, 0.7% Mn, 0.25% Si, and trace amounts of P and S. Each billet was machined to a diameter of 20 mm and a length of 60 mm before forging.

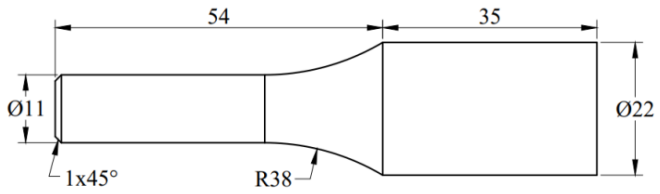

Fig. 1. Welding horn.

B. Hot Forging Setup

The forging process was conducted at the Mechanical Workshop (C1), Ho Chi Minh City University of Technology, using a 40-ton hydraulic press. Induction heating was performed with a MOSFET-Power GE-20 furnace. Five heating temperatures were selected: 1,220 °C, 1,232 °C, 1,247 °C, 1,266 °C, and 1,275 °C. These temperatures were based on literature recommendations for hot forging of medium-carbon steels (above 1,200 °C to ensure ductility and below ~1,280 °C to avoid grain coarsening and oxidation) and were further validated through preliminary heating trials. For clarity, the experimental conditions were: Horn 1 (control, no forging), Horn 2 (1,220 °C), Horn 3 (1,232 °C), Horn 4 (1,247 °C), Horn 5 (1,266 °C), and Horn 6 (1,275 °C).

Each billet was held at its target temperature for approximately 30 s to ensure thermal homogeneity, and it was immediately transferred to the press for hot forging using a closed-die extrusion configuration. The preliminary trials further confirmed that the short holding time was sufficient, as billets exhibited uniform color distribution and no measurable temperature gradient between surface and core. A commercial water-based graphite lubricant (Ramudo W144), containing approximately 20 wt.% graphite, 70 wt.% water, and minor stabilizers/additives, was applied to reduce friction and prevent die sticking during forging.

C. Heat Treatment

To preserve the effects of hot deformation on microstructure and acoustic behavior, no post-forging heat treatment (such as quenching or tempering) was applied. The influence of billet heating temperature alone on grain morphology, phase transformation, and ultrasonic properties was evaluated directly after forging.

Microstructural observations were performed using optical microscopy. The samples were sectioned at the shoulder, transition, and tip regions. They were mounted, ground with SiC papers up to 2,000 grit, polished with 1 μm alumina, and etched with 2% nital solution before imaging at 200× and 500× magnifications.

DRX was identified by the presence of fine, equiaxed grains with well-defined boundaries replacing elongated and deformed grains. The average grain size was measured using the linear intercept method according to the ASTM E112 standards, with at least 50 grains counted per region.

D. Forging Simulation

To better understand the thermomechanical behavior of the C45 billet during hot forging, a finite element simulation was performed using the DEFORM-3D software. This process aimed to visualize the progression of deformation, temperature distribution, velocity field, and stress concentration under realistic forging conditions. The billet geometry and die setup matched the experimental configuration, with temperature-dependent material properties and thermal-mechanical boundary conditions applied. A constant downward punch velocity, a die temperature of 250 °C, and billet heating temperatures ranging from 1,220 °C to 1,275 °C were considered. Frictional contact between the billet and die was defined using Ramudo W144 hot forging lubricant, and heat transfer coefficients were applied at the die-billet interface to account for cooling effects during forging.

E. Horn Fabrication

Based on the simulation outcomes, the horn geometry and forging parameters were optimized to achieve uniform deformation and favorable thermal distribution. Cylindrical C45 steel billets were heated to target temperatures ranging from 1,220 °C to 1,275 °C, as identified in the simulation. The billets were then forged using a single-stroke open-die press designed to replicate the deformation profile observed in the simulation. Forging was carried out promptly after removal from the furnace to minimize surface oxidation. The forged horns were subsequently cleaned using sandblasting to remove surface scale, reveal contour features, and turning, as shown in Figure 2. Acoustic performance was evaluated using a 28 kHz ultrasonic analyzer (XYZ model). The resonance frequency (F_a, F_r), cutoff frequency (F_c), acoustic impedance (Z_a, Z_r), and mechanical quality factor (Q_m) were recorded under free-vibration conditions.

Fig. 2. Forged horns after: (a) surface cleaning by sandblasting and (b) turning.

III. RESULTS AND DISCUSSION

A. Simulation Results

Figure 3 illustrates the simulation results of the hot forging process at the final forging stage (t = 1.15 s). In Figures 3(a) and 3(b), the temperature distribution and load prediction are presented. A significant thermal gradient was observed between the billet core and surface. The core temperature remained around 390 °C, while the outer regions cooled below 200 °C due to contact with the die. The corresponding forging load reached its peak at approximately 1.26×106 N, indicating a maximum material resistance during full cavity filling. These results suggest that sufficient heating is necessary to maintain core ductility and avoid surface hardening.

Figures 3(c) and 3(d) depict the velocity field and the time-dependent velocity response at 1.15 s. Material flow was strongly directed outward and upward near the die-billet interface, with maximum velocities exceeding 115 mm/s. The velocity-time curve showed a steep increase in surface velocity, reflecting accelerated deformation in peripheral regions. This unbalanced flow, if not thermally stabilized, may lead to uneven strain distribution and localized defects.

The stress response of the billet at the same forging stage is illustrated in Figures 3(e) and 3(f). The effective stress field exceeded 1,300 MPa near the die shoulder and the lower part of the billet, correlating with regions of intense deformation. Despite this stress accumulation, the core temperature remained relatively high, reducing the possibility of cracking. However, the drop in surface temperature combined with high stress magnitudes may lead to strain localization and microstructural anisotropy.

An overview of billet deformation is provided in Figures 3(g) and 3(h) through mesh distortion and temperature distribution at 0.914 s and 1.15 s. At t = 0.914 s, the billet was actively filling the die cavity, with elevated core temperature and localized deformation near the fillet. However, at t = 1.15 s, mesh elements near the die shoulder and base became severely compressed, indicating concentrated plastic strain. The corresponding temperature field showed a persistent gradient between the hot core and cooled surface, underscoring the importance of thermal management throughout the process.

In summary, the simulation revealed a strong interaction between mechanical deformation and thermal distribution during hot forging. Proper billet preheating improved cavity filling while minimizing surface hardening, stress concentration, and microstructural inconsistency. These results are consistent with previous simulation and experimental studies on medium-carbon steel forging [8, 9], confirming the reliability of the DEFORM-3D model as a predictive tool for optimizing process parameters and improving forging quality.

B. Microstructure Characterization

The experimental microstructural analysis was conducted to validate the deformation and thermal trends predicted by the DEFORM-3D simulation. Three longitudinal positions (labeled 1, 2, and 3) were selected on the transverse cross-section of the horn specimens (Figure 4), corresponding to the shoulder, transition, and tip regions of the forged part, respectively. Based on prior simulation and forging results, three representative samples - Horn 1 (non-forged control), Horn 3 (intermediate quality), and Horn 5 (optimal forging condition) - were chosen for microstructural examination at these positions.

Figure 5 illustrates the optical micrographs of Horn 1 at positions 1-3, representing the initial microstructure of the as-machined cylindrical billet. Figures 5(a), 5(c), and 5(e) correspond to 200× magnification, while Figures 5(b), 5(d), and 5(f) correspond to 500× magnification at the same positions. The microstructure revealed coarse, elongated grains with no evidence of DRX. The presence of flow lines was minimal, and the grain boundaries remained intact and oriented along the rolling direction. Position 1, located near the shoulder region, exhibited a slightly more irregular grain shape due to the machining effects, but no deformation-induced refinement was observed. Overall, Horn 1 retained the as-received structure typical of hot-rolled and annealed C45 steel, serving as a reference for comparison with forged samples. The lack of plastic deformation in this control sample made it useful for identifying microstructural evolution due to forging in subsequent samples.

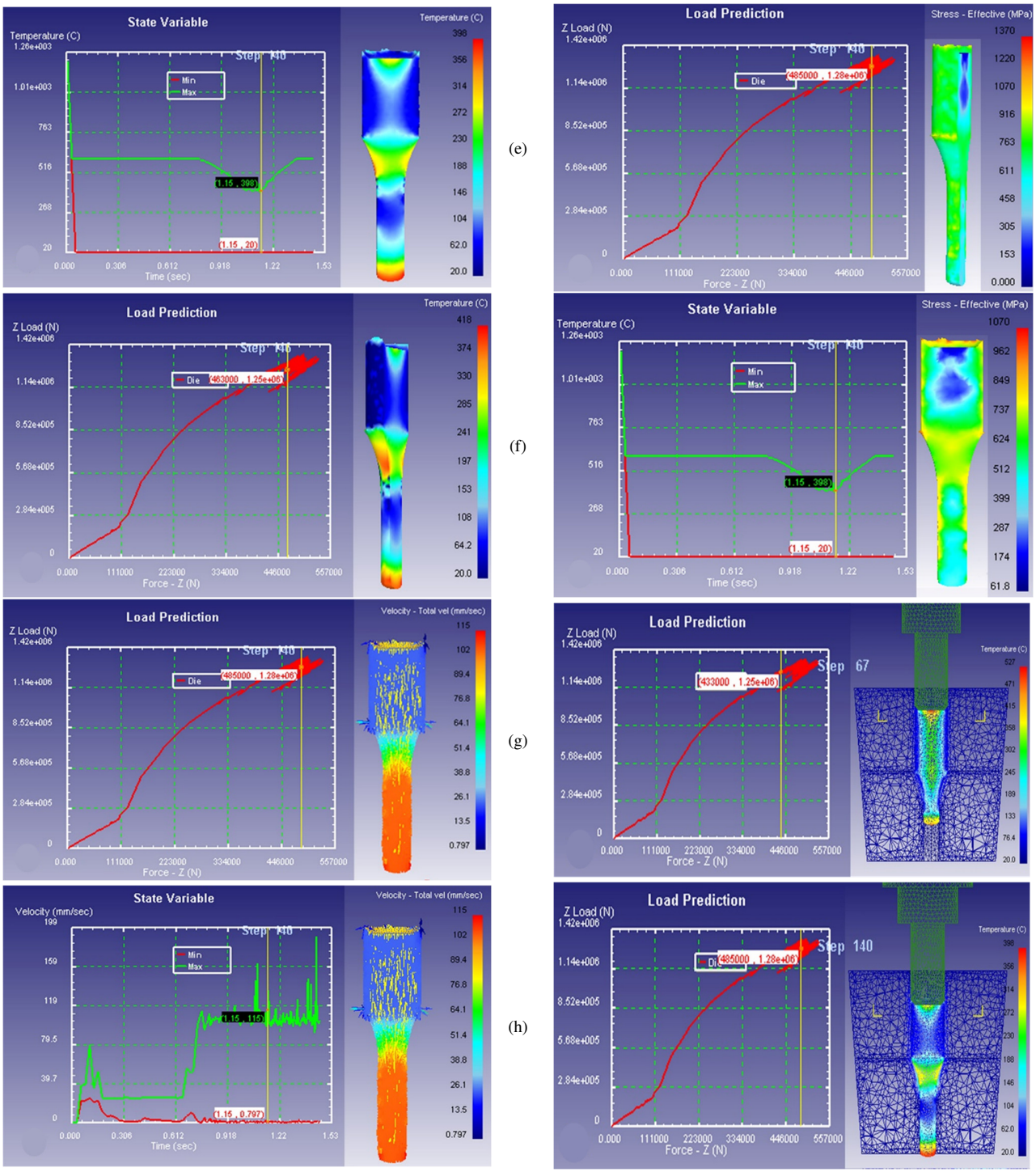

Fig. 3. Simulation results of the hot forging process at t = 1.15 s. (a) Temperature distribution, (b) Forging load curve, (c) Velocity field, (d) Velocity-time plot, (e) Effective stress field, (f) Stress-temperature map and billet deformation progression, (g) Mesh and temperature at t = 0.914 s, and (h) Mesh and temperature at t = 1.15 s.

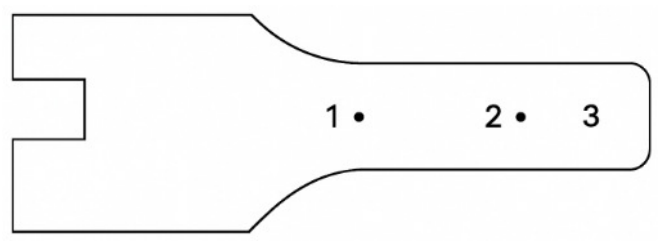

Fig. 4. Sampling positions for microstructural analysis on the transverse cross-section of the horn specimen.

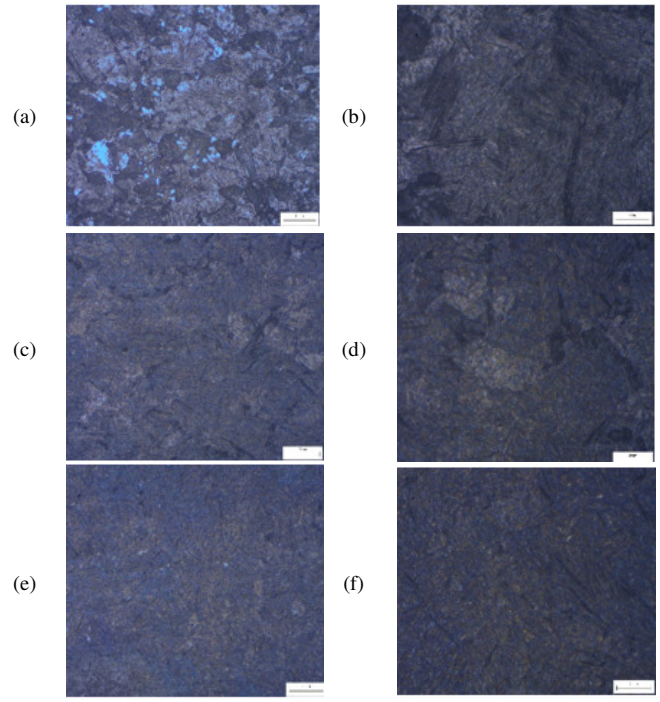

Fig. 5. Optical microstructure of Horn 1 at positions 1-3 on the transverse cross-section, with magnifications of 200× (a), (c), and (e), and 500× (b), (d), and (f).

Figure 6 depicts the microstructure of Horn 3 at three longitudinal positions with magnifications of 200× and 500×. Compared to the control specimen, Horn 3 revealed moderate microstructural refinement due to hot forging at ~1,232 °C. At positions 1 and 2, elongated grains with partially fragmented boundaries indicated incomplete DRX. The average grain size remained coarse (~38-42 µm), and residual deformation zones were still visible. At position 3 (tip region), finer and more equiaxed grains (~26 µm) suggested localized DRX, where plastic strain was more concentrated. In contrast, Horn 1 exhibited uniform elongated grains with no DRX, and grain size exceeded 50 µm throughout. The ultrasonic resonance testing of Horn 3 revealed a resonant frequency of 19.6 kHz and a Q-factor of 2,250, both of which were lower than those of Horn 5 (20.0 kHz and Q = 3,450, respectively). The lower Q-factor reflected higher internal damping, likely caused by microstructural heterogeneity and incomplete recrystallization. Compared to the control Horn 1 (non-resonant or extremely low Q < 1,000), Horn 3 showed significant improvement in wave transmission but remained suboptimal for ultrasonic horn performance. These findings highlighted that forging at 1,232 °C could initiate beneficial microstructural changes, but both DRX and grain homogeneity were insufficient for optimal acoustic efficiency. Higher forging temperatures were necessary to balance mechanical and ultrasonic properties, consistent with prior findings that DRX dominated above 1,250 °C in medium-carbon steels [16, 20].

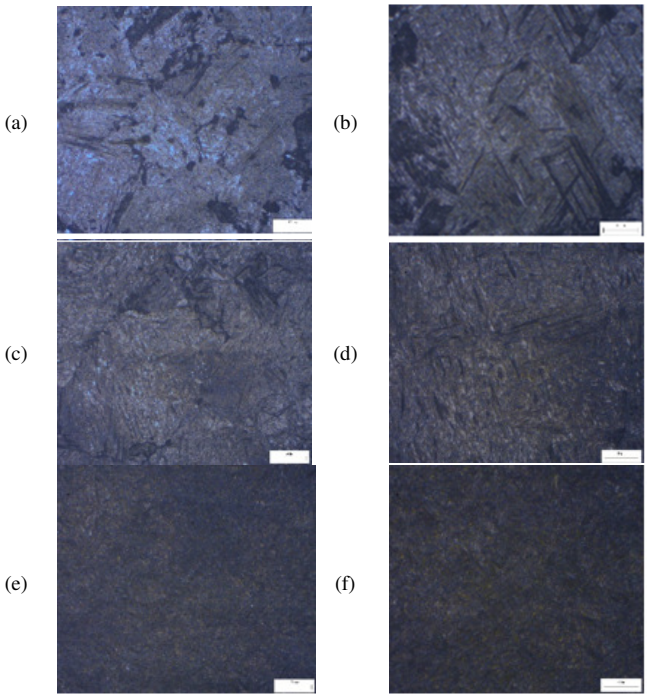

Fig. 6. Optical microstructure of Horn 3 at positions 1-3 on the transverse cross-section, with magnifications of 200× (a), (c), and (e), and 500× (b), (d), and (f).

Figure 7 presents the microstructure of Horn 5 at positions 1-3, observed under 200× and 500× magnifications. Horn 5, forged at approximately 1,266 °C, exhibited a fully DRX microstructure, characterized by fine, equiaxed grains uniformly distributed across the cross-section. The average grain size ranged from 15 to 18 µm, with position 3 showing the finest grains (~15 µm) due to higher local deformation. Clear grain boundaries and the absence of elongated or uncrystallized regions indicated that the thermal and strain conditions during forging were sufficient to activate complete DRX throughout the specimen. Compared to the other two samples, Horn 5 demonstrated A significantly refined microstructure, achieving the optimum acoustic response, with a resonance frequency of 20.0 kHz and a quality factor of 3,450. In contrast, Horn 3 resonated at 19.6 kHz with Q = 2,250, reflecting greater wave scattering due to microstructural inhomogeneity and residual stress, while Horn 1, with its coarse and anisotropic grain structure, exhibited poor ultrasonic performance with Q < 1,000, unable to sustain strong resonance. These findings confirmed a strong correlation between microstructure and acoustic behavior: refined and homogeneous DRX structures reduce internal scattering and enhance ultrasonic efficiency, critical for applications like

ultrasonic transducers. Table I summarizes the grain size of the three samples at each position.

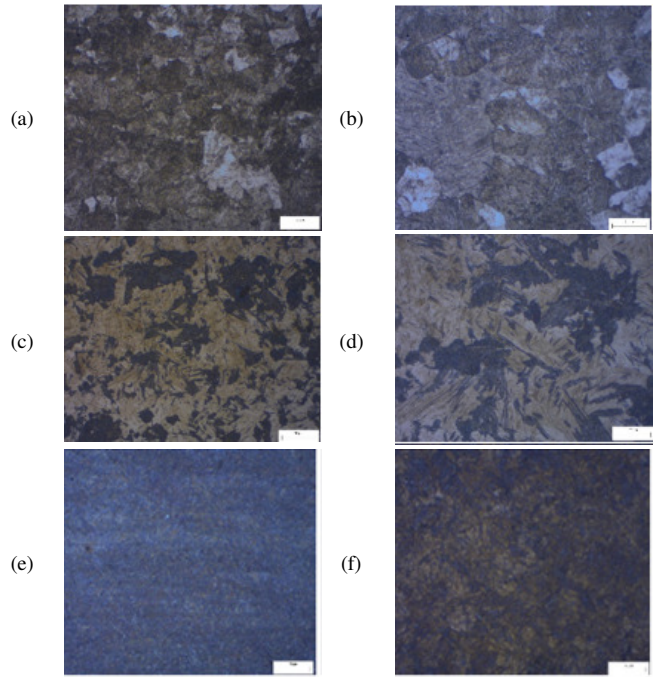

Fig. 7. Optical microstructure of Horn 5 at positions 1-3 on the transverse cross-section, with magnifications of 200× (a), (c), and (e), and 500× (b), (d), and (f).

TABLE I. GRAIN SIZE SUMMARY OF REPRESENTATIVE HORN SAMPLES (1, 3, AND 5) AT THREE POSITIONS

Horn	Forging temperature (°C)	Grain size, µm			Remarks
		Position 1	Position 2	Position 3	
1	-	> 50	> 50	> 50	No DRX, elongated grains
3	1,232	38-42	38-42	~26	Partial DRX, heterogeneous
5	1,266	18-20	16-18	~15	Full DRX, homogeneous

C. Ultrasonic Resonance and Acoustic Performance

The acoustic characteristics of all forged and control specimens were measured using a 28 kHz ultrasonic analyzer. Parameters, such as resonance frequency (F_a, F_r), cutoff frequency (F_c), acoustic impedance (Z_a and Z_r), and mechanical quality factor (Q_m), were obtained to evaluate the energy transfer efficiency and wave propagation stability (Table II). Each acoustic test was repeated three times under identical conditions, and the values of resonance frequency, impedance, and Q-factor were averaged. The control sample (Horn 1) exhibited the highest Q_m value of 3,434. This indicates that it had the lowest internal energy loss and was the most efficient at transmitting ultrasonic energy under free-vibration test conditions. However, under ultrasonic excitation, the control sample showed localized heating and burning at the antinode region (Figure 2(b)). This can be attributed to its coarse and anisotropic grain structure, which promotes stress concentration and uneven energy dissipation at the horn belly, ultimately leading to thermal failure. Forged horns (Horns 2-6) showed a lower Q_m compared to the control sample by 30-40%. Specifically, Horns 3 and 4, processed at 1,232 and 1,247 °C, demonstrated the lowest Q_m and acoustic impedance values, while Horn 5 showed the highest Q_m among the forged specimens, indicating that 1266 °C is the optimal temperature for minimizing the acoustic degradation caused by forging.

TABLE II. TEST DATA WITH 28 KHZ FREQUENCY OF 6 HORNS

Samples	F_a (Hz)	F_c (Hz)	F_r (Hz)	Z_a	Z_r	Q_m
Horn 1	28,009	27,898	27,786	37.05	13.3	3,434
Horn 2	27,590	27,484	27,378	25.41	22.3	2,144
Horn 3	27,484	27,376	27,273	14.92	15.9	2,031
Horn 4	27,611	27,506	27,400	27.37	26.1	2,020
Horn 5	27,694	27,593	27,492	26.4	22.5	2,340
Horn 6	27,501	27,399	27,297	18.62	15.9	2,263

The variations in F_a, F_c, and F_r are depicted in Figure 8. Horn 1 maintained the highest frequency values across all parameters, while the forged samples showed a downshift in resonance, likely due to grain misalignment and induced anisotropy during forging. The frequency decay trends presented in Figure 9 demonstrated that Horn 5 experienced the fastest damping, leading to lower signal stability.

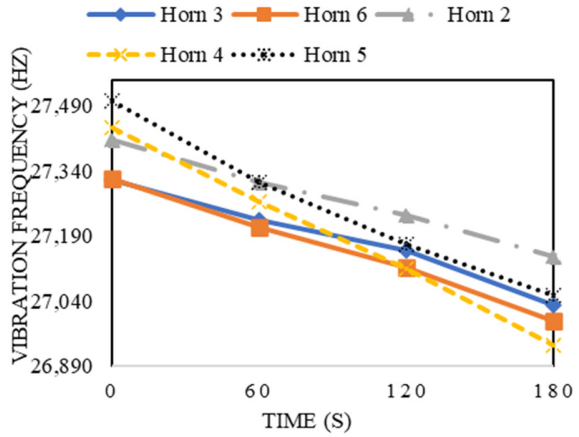

Fig. 8. Frequency variation F (Hz) over 6 horns.

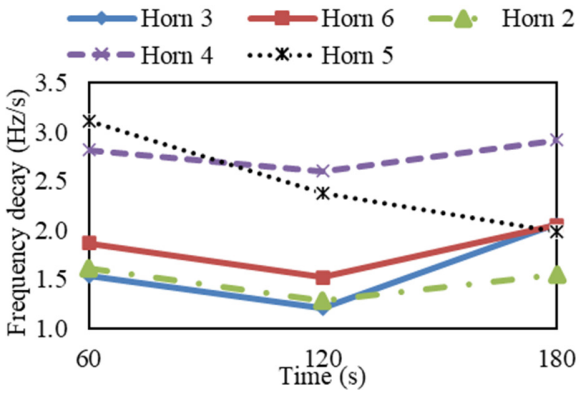

Fig. 9. Frequency decay rate of the horns over time.

D. Correlation between Microstructure and Transmission Efficiency

The acoustic performance of the horns was strongly affected by their microstructure, further depended on billet heating temperature. Within the temperature range of 1,247-1,266 °C, DRX promoted refined grains and reduced anisotropy, improving wave transmission (as in Horn 5). In contrast, coarse or uneven pearlite colonies led to lower Q_m and impedance values.

These findings are consistent with previous reports that finer and more homogeneous grains led to reduced ultrasonic attenuation and improved resonance stability [14, 22]. In particular, the complete DRX observed in Horn 5 at 1,266 °C, which explains the higher *Q*-factor, agreed with the findings of [21], where microstructural uniformity enhanced acoustic efficiency. This correlation highlights the practical importance of controlling billet heating temperature to achieve predictable horn performance for industrial ultrasonic welding applications.

Although hot forging significantly enhances mechanical properties through strain hardening and DRX, it can compromise acoustic efficiency if microstructural anisotropy is not controlled. Therefore, a balanced heating temperature - sufficient for grain refinement but not excessive to induce orientation gradients - is essential for producing steel ultrasonic horns with both mechanical integrity and stable resonance behavior.

IV. CONCLUSION

This study investigated the influence of billet heating temperature on the microstructure and ultrasonic transmission efficiency of hot-forged C45 steel horns. Based on the experimental and microstructural analyses, the following conclusions are drawn:

- Billet heating temperature critically influenced grain morphology, hardness, and acoustic behavior.
- The unforged control horn (Horn 1), while exhibiting the highest mechanical quality factor (Q_m), in free-vibration tests, suffered a thermal failure under ultrasonic operation.
- Among the forged horns, Horn 5 (1266 ºC) exhibited the best acoustic performance. It also produced a fully Dynamically Recrystallized (DRX) microstructure with a grain size of 15-18 μm.
- The forging process reduced the Q_m value compared to the unforged state, but it was necessary to ensure thermal stability under operational loads.

FUNDING

This research was funded by the Vietnam National University Ho Chi Minh City (VNU-HCM) under grant number: B2023-20-13.

REFERENCES

[1] K. F. Graff, "Ultrasonic metal forming: materials," in *Power Ultrasonics*, J. A. Gallego-Juárez and K. F. Graff, Eds. Sawston, UK: Woodhead Publishing, 2015, pp. 337–376.

[2] A. Yusefi, A. H. Kokabi, R. Abedini, V. Fartashvand, and V. Allahverdizadeh, "Microstructure evolution and mechanical properties analysis in dissimilar ultrasonic metal welding of aluminum to copper," *Journal of Materials Research and Technology*, vol. 30, pp. 2922–2935, May 2024, https://doi.org/10.1016/j.jmrt.2024.04.037.

[3] Z. Liu, Y. Li, W. Liu, H. Zhou, S. Ao, and Z. Luo, "Enhancing the ultrasonic plastic welding strength of Al/CFRTP joint via coated metal surface and structured composite surface," *Journal of Manufacturing Processes*, vol. 108, pp. 227–237, Dec. 2023, https://doi.org/10.1016/j.jmapro.2023.11.001.

[4] T.-H. Nguyen, L. T. Nguyen, T. M. Quynh Tran, N. H. Nguyen, and V. T.-T. Chung, "Analysis of process parameters of hypoeutectoid steel ultrasonic horns with different heat treatment processes," *Japanese Journal of Applied Physics*, vol. 60, no. 12, Aug. 2021, Art. no. 126502, https://doi.org/10.35848/1347-4065/ac3727.

[5] Z.-J. Bao *et al.*, "Development Trend in Composition Optimization, Microstructure Manipulation, and Strengthening Methods of Die Steels under Lightweight and Integrated Die Casting," *Materials*, vol. 16, no. 18, Sept. 2023, Art. no. 6235, https://doi.org/10.3390/ma16186235.

[6] S. Madhankumar *et al.*, "Study and selection of hot forging die materials and hardness," *Materials Today: Proceedings*, vol. 45, pp. 6563–6566, 2021, https://doi.org/10.1016/j.matpr.2020.11.472.

[7] A. A. Emamverdian, Y. Sun, C. Cao, C. Pruncu, and Y. Wang, "Current failure mechanisms and treatment methods of hot forging tools (dies) - a review," *Engineering Failure Analysis*, vol. 129, Nov. 2021, Art. no. 105678, https://doi.org/10.1016/j.engfailanal.2021.105678.

[8] M. Davoudi, A. F. Nejad, S. S. Rahimian Koloor, and M. Petrů, "Investigation of effective geometrical parameters on wear of hot forging die," *Journal of Materials Research and Technology*, vol. 15, pp. 5221–5231, Nov. 2021, https://doi.org/10.1016/j.jmrt.2021.10.093.

[9] R. Rajiev, P. Sadagopan, and R. Shanmuga Prakash, "Study on investigation of hot forging die wear analysis – An industrial case study," *Materials Today: Proceedings*, vol. 27, pp. 2752–2757, 2020, https://doi.org/10.1016/j.matpr.2019.11.330.

[10] B. Chandra Kandpal *et al.*, "Effect of heat treatment on properties and microstructure of steels," *Materials Today: Proceedings*, vol. 44, pp. 199–205, 2021, https://doi.org/10.1016/j.matpr.2020.08.556.

[11] M. Asif, M. A. Ahad, M. F. H. Iqbal, and S. Reyaz, "Experimental investigation of thermal properties of tool steel and mild steel with heat treatment," *Materials Today: Proceedings*, vol. 45, pp. 5511–5517, 2021, https://doi.org/10.1016/j.matpr.2021.02.272.

[12] X. Xu *et al.*, "Structure-Property Relationship in a Micro-laminated Low-Density Steel for Offshore Structure," *Steel research international*, vol. 90, no. 5, 2019, Art. no. 1800515, https://doi.org/10.1002/srin.201800515.

[13] J. Kusiak and R. Kuziak, "Modelling of microstructure and mechanical properties of steel using the artificial neural network," *Journal of Materials Processing Technology*, vol. 127, no. 1, pp. 115–121, Sept. 2002, https://doi.org/10.1016/S0924-0136(02)00278-9.

[14] J. L. Tai, M. T. H. Sultan, A. Łukaszewicz, F. S. Shahar, W. Tarasiuk, and J. Napiórkowski, "Ultrasonic Velocity and Attenuation of Low-Carbon Steel at High Temperatures," *Materials*, vol. 16, no. 14, July 2023, Art. no. 5123, https://doi.org/10.3390/ma16145123.

[15] J. Zhou, H. Liao, H. Chen, and A. Huang, "Effects of hot-forging and subsequent annealing on microstructure and mechanical behaviors of Fe35Ni35Cr20Mn10 high-entropy alloy," *Materials Characterization*, vol. 178, Aug. 2021, Art. no. 111251, https://doi.org/10.1016/j.matchar.2021.111251.

[16] F. Zhao, H. Hu, X. Liu, Z. Zhang, and J. Xie, "Effect of billet microstructure and deformation on austenite grain growth in forging heating of a medium-carbon microalloyed steel," *Journal of Alloys and Compounds*, vol. 869, July 2021, Art. no. 159326, https://doi.org/10.1016/j.jallcom.2021.159326.

[17] J. Sarkar, P. Modak, S. B. Singh, and D. Chakrabarti, "Effect of cooling-rate during solidification on the structure-property relationship of hot deformed low-carbon steel," *Materials Chemistry and Physics*, vol. 257, Jan. 2021, Art. no. 123826, https://doi.org/10.1016/j.matchemphys.2020.123826.

[18] Q. Yang, Y. Zhou, W. Zhang, X. Zhang, and M. Xu, "Effect of Ultrasonic-Assisted Casting on Hot Deformation Mechanism and Microstructure of 35CrMo Steel Ingot," *Materials*, vol. 15, no. 1, 2022, Art. no. 146, https://doi.org/10.3390/ma15010146.

[19] A. Sourav, S. Yebaji, and S. Thangaraju, "Structure-property relationships in hot forged AlxCoCrFeNi high entropy alloys," *Materials Science and Engineering: A*, vol. 793, Aug. 2020, Art. no. 139877, https://doi.org/10.1016/j.msea.2020.139877.

[20] B. G. Prusty and A. Banerjee, "Structure–Property Correlation and Constitutive Description of Structural Steels during Hot Working and Strain Rate Deformation," *Materials*, vol. 13, no. 3, Jan. 2020, Art. no. 556, https://doi.org/10.3390/ma13030556.

[21] S. T. Abraham, S. Shivaprasad, C. R. Das, S. K. Albert, B. Venkatraman, and K. Balasubramaniam, "Characterisation of heterogeneous microstructure in large forged products using nonlinear ultrasonic method," *Materials Science and Technology*, vol. 36, no. 6, pp. 699–708, Apr. 2020, https://doi.org/10.1080/02670836.2020.1732077.

[22] T. Wan, T. Naoe, T. Wakui, M. Futakawa, H. Obayashi, and T. Sasa, "Effects of Grain Size on Ultrasonic Attenuation in Type 316L Stainless Steel," *Materials*, vol. 10, no. 7, July 2017, Art. no. 753, https://doi.org/10.3390/ma10070753.